Appendix A

Study of Errors in Conductivity Meters Using the Low Induction Number Approximation and How to Overcome Them

F.C.M. Andrade, T. Fischer and J. Valenta

22nd European Meeting of Environmental and Engineering Geophysics

EAGE - Near Surface Geoscience, Barcelona, Spain, Extended Abstracts. 2016

DOI: 10.3997/2214-4609.201602080

We 22P2 24

Study of Errors in Conductivity Meters Using the Low Induction Number Approximation and How to Overcome Them

F.C.M. Andrade* (Charles University in Prague), T. Fischer (Charles University in Prague) & J. Valenta (Charles University in Prague)

SUMMARY

In this contribution we made a study of the errors in obtaining the apparent electrical conductivity of the earth by electromagnetic induction conductivity meters which use the low induction number (LIN) approximation. We have made theoretical simulations, using the full Maxwell's equations, of conductivity measurements at any height from the ground using the technical specifications of several known brands of conductivity meters, and calculated the observed errors in the measurements for a wide range of ground conductivities in order to achieve the accuracy of the use of the LIN approximation for the calculation of the apparent conductivity and propose other simple but more accurate methods to calculate the apparent conductivity from the mutual coupling ratio (Q) which is measured by the conductivity meters.

Introduction

Electromagnetic induction (EMI) techniques are widely used to obtain subsurface apparent electrical conductivity (σ_a) as they can be easily operated allowing to explore large areas in a short period of time. EMI methods, can be used for a wide range of applications and notably to soil mapping, contaminants detection, characterization of shallow aquifers, location of buried objects and ore bodies.

The EMI equipments consists basically in a primary magnetic field transmitter (coil) and, depending on the brand, a single or a set of magnetic field receivers. Measurements can be performed in several coil configurations but the two mostly used are the vertical dipole mode or horizontal coplanar loops (HCP) and the horizontal dipole modes or vertical coplanar loops (VCP). Measurements with the vertical dipole mode have a higher depth penetration than with the horizontal dipole. As a rule of thumb, horizontal dipoles (VCP) loops sense the ground up to a depth of approximately 0.75 times the coil separation while vertical dipoles (HCP) loops sense depth levels of approximately 1.5 times the coil offset. Other factors influencing the EMI penetration depth are the instrument height above the surface and the operating frequency.

Several EMI commercial instruments, namely the ones called conductivity meters, measure the mutual coupling ratio (Q) which is the ratio between the secondary magnetic field (H^S), induced by the ground, and the primary magnetic field (H^p), which corresponds to the direct wave propagating from the transmitter through the air, at the receiver coil and use the so called *Low Induction Number* (LIN) approximation, described in McNeill (1980), in which a linear relationship between the measured off-phase component of Q is used to calculate the apparent conductivity.

In this paper we made theoretical simulations, using the full Maxwell's equations and the technical specifications of several known brands of conductivity meters, to achieve the accuracy of the use of the LIN approximation for the calculation of the apparent conductivity (σ_a) and propose other simple but more accurate methods to calculate σ_a

Theory and methodology

The Maxwell-based full solution for the magnetic field measured over a horizontal layered medium is given by Keller and Frischknecht (1966) and Anderson (1979). The geophysical instruments generally measure the ratio between the secondary and the primary magnetic field at the receiver coil. This quantity is called the mutual coupling ratio (Q).

The electromagnetic forward model for horizontal and vertical dipole source-receiver combination with an intercoil separation $\boldsymbol{s}$ over an 1-D layered earth with N layers over an infinite half-space with conductivity σ_{N+1}, can be written as:

$$Q^{HCP}(s)=\frac{H_Z^S}{H_Z^P}=\frac{H_Z-H_Z^P}{H_Z^P}=-s^3\int_0^\infty R_0(\lambda)J_0(s\lambda)\lambda^2\,d\lambda \quad (1)$$

$$Q^{VCP}(s)=-s^2\int_0^\infty R_0(\lambda)J_1(s\lambda)\lambda\,d\lambda \quad (2)$$

where J_0 and J_1 are the first kind zero-order and first-order Bessel functions, λ is the radial wave number and. $R_0(\lambda)$ is called the reflection factor calculated at the interface between the air and the first layer, and can be obtained recursively beginning with the bottom layer N observing that there are no upcoming waves from the lower half-space, so $R_{N+1}=0$ and:

$$R_n(\lambda)=\frac{(\Gamma_n-\Gamma_{n+1})/(\Gamma_n+\Gamma_{n+1})+R_{n+1}e^{-2\Gamma_{n+1}h_{n+1}}}{1+(\Gamma_n-\Gamma_{n+1})/(\Gamma_n+\Gamma_{n+1})R_{n+1}e^{-2\Gamma_{n+1}h_{n+1}}}\quad , \quad (3)$$

where $\Gamma_n=\sqrt{\lambda^2+i\omega\mu_0\sigma_n}$, h_n is the thickness, μ_0 is the permeability of vacuum, ω is the angular frequency and σ_n is the electrical conductivity of the n^{th} layer. $R_0(\lambda)$ is obtained assuming layer 0 as the

air with $\sigma_0 = 0$. We can easily use the above methodology also to compute Q when the equipment is used at some height (h_e) from the ground over a homogeneous earth considering the model as composed by one single infinity layer with the conductivity of the ground bellow an air layer with $\sigma=0$ and thickness h_e. The integrals in equations (1) and (2), the Hankel transforms of functions $\lambda^2 R_0$ and λR_0, respectively, can be calculated by linear filtering. Here we used the Guptasarma and Singh (1997) filters with 120 elements for the Hankel J_0 transform and 140 elements for the Hankel J_1 transform.

So the problem is set to how to compute the apparent conductivity, which is the conductivity of an equivalent homogeneous media that should lead to the same values of Q measured by the equipments or computed for the layered model using the above described methodology in synthetic data. Using the low induction number (LIN) approximation, the following equation for a homogeneous half-space for coils directly over the surface of the ground (Mcneill, 1980) is valid:

$$\sigma_a \simeq \frac{4}{\omega \mu_o s^2} \Im\left(\frac{H_S}{H_p}\right)^{VCP} \simeq \frac{4}{\omega \mu_o s^2} \Im\left(\frac{H_S}{H_p}\right)^{HCP} \quad . \tag{4}$$

This equation should lead to good approximations only when the induction number (***B***), defined as the ratio between the intercoil separation (***s***) and the skin depth, defined as $\delta = \sqrt{2/(\omega \mu_o \sigma)}$ of the homogeneous medium, is much smaller than 1, (***B***<<1). Note that the LIN approximation (4) is derived from an analytical equation for coils laid directly over the surface of the ground and leads to some additional errors if the coils are at some height from the surface. So using equation (4), we can easily obtain the expressions for the apparent conductivity for vertical and horizontal dipoles using the imaginary part (Off-Phase component) of Q given in equations (1) and (2).

Our analysis of the errors observed when using the LIN approximation is then made by calculating the apparent conductivity by equations (1), (2), (3) and (4) for several values of ground conductivity in our homogeneous model using the technical parameters of some widely used commercial conductivity meters. Obviously both values of conductivity (the used in calculations and the resultant obtained value) should be equal or very similar if the condition of the LIN approximation is fulfilled (***B***<<1). So, comparing both values we can verify if the LIN approximation is being properly used by these equipments and consequently if they present satisfactory values of the apparent conductivities.

Results

We have made error analysis for the Geonics EM-31-MK2, EM-34-3, which can measure at three different intercoil spacing, and for the GF Instruments CMD-Explorer which measures at three different intercoil spacing at the same time. The technical specifications of these equipments are shown in Table 1. For the lack of space we will present here just the more critical error situations for the three equipments analysed.

In Figure 1 we show the plots for the apparent conductivity (σ_a) obtained by LIN approximation *versus* ground conductivity as well as the percentage errors for the CMD-Explorer, s = 4.49m for HCP and VCP configurations for the equipment laid in the ground and carried at a typical height (h_e) of 1m. In Figure 2 we show the same plots for the Geonics EM-31-MK2.

Instrument	Intercoil spacing(s) (m)	Frequency(ies) (Hz)
Geonics EM-31-MK2	3.66	9800
Geonics EM-34-3	10 – 20 – 40	6400 – 1600 - 400
CMD-Explorer	1.48 – 2.82 – 4.49	10000

Table 1 *– Technical specifications of the conductive meters analysed.*

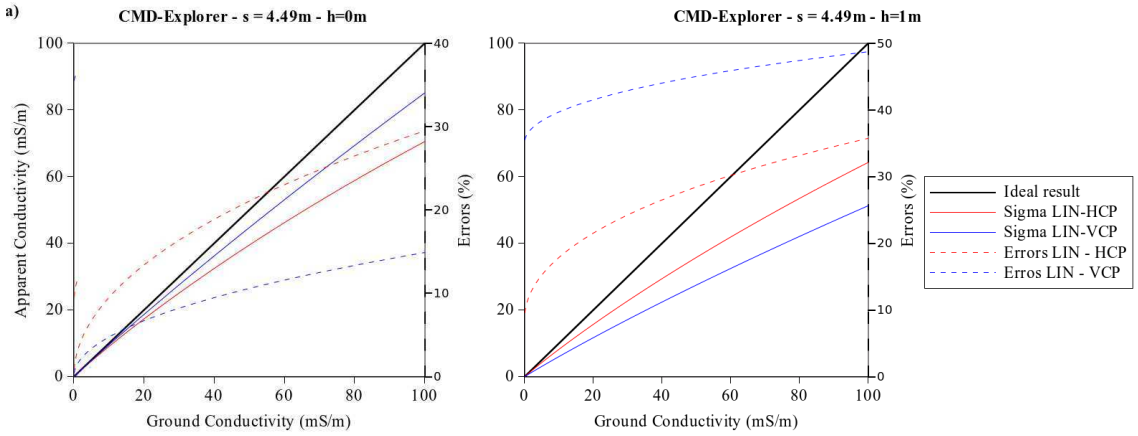

***Figure 1**. Apparent conductivity (σ_a) obtained by LIN approximation and percentage errors for the CMD-Explorer, **s** = 4.49m for HCP and VCP configurations. a) h_e = 0 and b) h_e = 1m.*

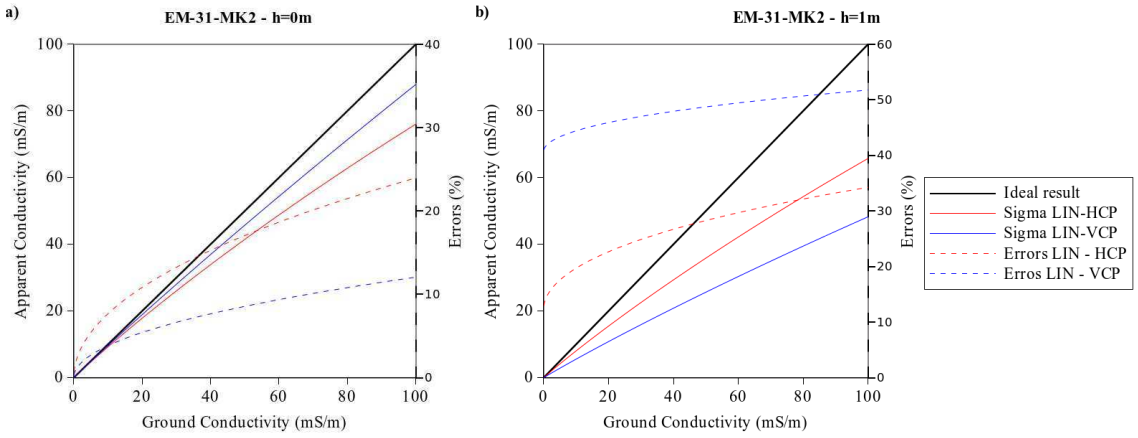

***Figure 2.** Apparent conductivity (σ_a) obtained by LIN approximation and percentage errors for the EM-31-MK2, s = 3.66m for HCP and VCP configurations. a) h_e = 0 and b) h_e = 1m.*

In Figure 3 we show the plots for EM-34-3 for HCP and VCP configurations with intercoil separations of 10 and 40 m. In the VCP configuration h_e=0.5m and for HCP, h_e=0m.

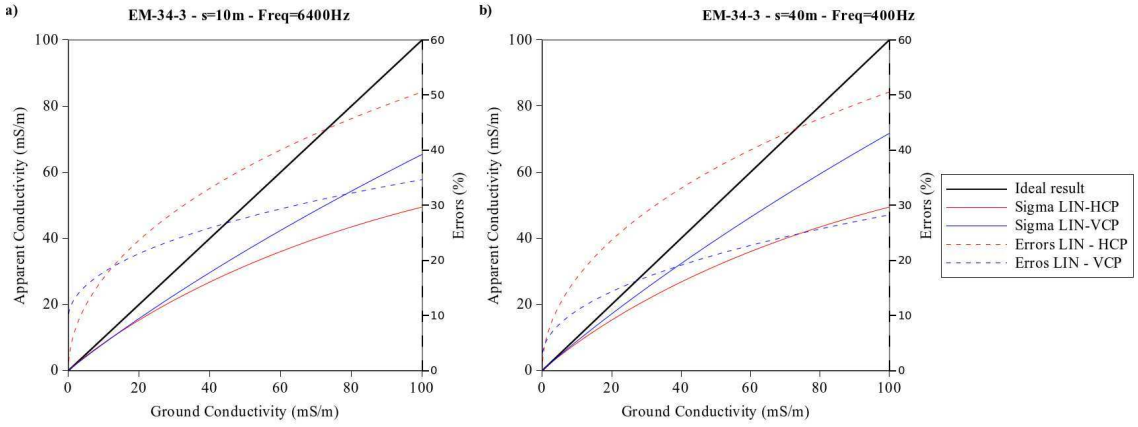

***Figure 3.** Apparent conductivity (σ_a) obtained by LIN approximation and percentage errors for the EM-34-3, for HCP and VCP configurations. a) s=10m and b) s=40m.*

We can see in Figures 1 and 2 that the errors are smaller for the horizontal dipole (VCP) when the equipment is lying on the ground but the situation inverts when the equipment is held at the height of 1m from the ground. This behaviour can be explained by the fact that for the horizontal dipole the depth of investigation is smaller than for the vertical dipole, so it is more affected by the air layer.

The manufactures of the CMD-Explorer claims that their equipment operates in the LIN zone but they do not use the LIN approximation equations, but instead they calibrate their measurements over some environments with known conductivities and the results given are calculated using a linear relationship constructed over these measurements. This does not seem to be a good solution as we can perfectly see that the behaviour or the error is not linear.

To overcome these problems we propose that equations (1), (2) and (3) can be used to find a ground conductivity (σ) value that leads to the same, or very similar, measured values of Q. In other words this problem can be solved by looking for a value of conductivity that minimizes the following function : $f(\sigma)=|Q^{obs}-Q^{mod}(\sigma)|$, where $Q^{mod}(\sigma)$ can be computed as described above. As it is a single variable (σ) the minimization of $f(\sigma)$ can be done by a simple or progressive direct search. For most situations found in nature, for example, conductivities smaller than 1S/m, we can use only the off-phase part of Q and find the root (zero) of the following equation: $g(\sigma)=(\Im(Q^{obs})-\Im(Q^{mod}(\sigma)))$ by the Newton-Rhapson method, which starting from an initial guess of σ_0 (in our case we can use the apparent conductivity obtained by the low induction number approximation) finds successively better approximations of the root of $g(\sigma)$ until a sufficiently small value is reached.

Conclusions

From the results shown above we can conclude that the calculations of the apparent conductivities by the LIN approximation diverge from the ideal curve even at low inductions numbers. In average, to obtain an error less than 5%, the induction number should be at least smaller then 0.05 for the case when the equipment is used over the ground. For the cases where the equipment is used at the height of 1m from the ground the error is never smaller than 20%. The errors observed for very commonly found values of conductivities in nature, for example 10mS/m, have a minimum value of 7.7% and a maximum of 44%.

So we saw that the equipments studied frequently do not operate in the Low Induction Number zone and they should not use the LIN approximation equation or any other linear calibration. We proposed another very simple methodology, which we think that with the nowadays very small and fast processors that can be used in hand-held equipments, could be easily implemented and would lead to much smaller errors in the computation of the apparent conductivity.

References

Anderson, W.L. [1979] Numerical-integration of related Hankel transforms of orders 0 and 1 by adaptive digital filtering. *Geophysics*, 44(7), 1287–1305.

Guptasarma, D. and Singh, B. [1997] New digital linear filters for Hankel J_0 and J_1 transforms. *Geophysical Prospecting*, 1997, 45, 745–762

Keller, G. and Frischknecht, F. [1966] Electrical methods in geophysical prospecting. *International series of monographs in electromagnetic waves 10*. Pergamon Press, Oxford, New York.

McNeill, J.D. [1980] Electromagnetic terrain conductivity measurement at low induction numbers. *Geonics Limited Technical Note TN-6*, Ontario.

Appendix B

Generalised relative and cumulative response functions for electromagnetic induction conductivity meters operating at low induction numbers

F.C.M. Andrade and T. Fischer

Geophysical Prospecting 66(3):595-602, 2018

DOI: 10.1111/1365-2478.12553

Geophysical Prospecting

EAGE EUROPEAN ASSOCIATION OF GEOSCIENTISTS & ENGINEERS

Geophysical Prospecting, 2018, **66**, 595–602 doi: 10.1111/1365-2478.12553

Generalised relative and cumulative response functions for electromagnetic induction conductivity meters operating at low induction numbers

Fernando César Moura de Andrade[1,2]* and Tomáš Fischer[1]

[1]*Faculty of Science, Institute of Hydrogeology, Engineering Geology and Applied Geophysics, Charles University, 128 43, Prague, and* [2]*Fundação Cearense de Meteorologia e Recursos Hídricos, Fortaleza, 60.115-221, Brazil*

Received March 2017, revision accepted July 2017

ABSTRACT

Relative and cumulative analytical response functions have been widely used as a powerful tool for forward modelling and interpretation of measurements obtained by electromagnetic induction conductivity meters operating at low induction numbers for one-dimensional layered earth models. These well-known functions were derived and should be used for the instruments laid on the surface of the earth. In this paper, we extended the response functions and obtained new generalised analytical expressions, which can be used for instruments carried at any height from the surface. The proposed new equations were compared with numerically constructed functions, obtained using the full solution of Maxwell's equations, and proved to be in very good agreement at low induction numbers. Quantitative analyses of the behaviour of the relative response and the depth of investigation of electromagnetic induction instruments, when raised from the ground, could also be done using the generalised functions.

Key words: Electromagnetic terrain conductivity measurements, Sensitivity, Electromagnetic modelling.

INTRODUCTION

One of the most commonly used geophysical techniques for mapping the electrical conductivity of the subsurface, in a fast and easy way, is by means of conductivity meters using the electromagnetic induction (EMI) principle. EMI methods can be used for a wide range of applications and notably for soil mapping, contaminant detection, characterisation of shallow aquifers, and location of buried objects or ore bodies. Recently, Babacan, Sahin and Cinar (2016) used the technique to investigate seawater intrusions in the eastern shore of the Black Sea. Martini *et al.* (2015) mapped soil moisture using repeated EMI measurements, and Hulin *et al.* (2015) applied the method to delineate an archaeological site. The EMI equipment, which is often called conductivity meter, consists basically of a primary magnetic field transmitter (coil) and, depending on the brand, a single or a set of magnetic field receivers. Measurements can be performed in several dipole modes, but the two mostly used are the vertical and horizontal dipoles in the horizontal coplanar (HCP) and vertical coplanar (VCP) coil configurations, respectively.

Relative response functions, also termed sensitivities curves, have been studied in several different ways, both using the full solution of Maxwell's equations or approximations for some specific range of frequencies, conductivities, or source–receiver distances, for example, the low induction number (LIN) approximation. For example, Callegary, Ferré and Groom (2007) compared the vertical spatial sensitivity for two-layered soil models using the one-dimensional (1D) solution of Maxwell's equations and the LIN approaches, and Guillemoteau *et al.* (2015) constructed 1D sensitivity curves using the Fréchet kernel computed for the equivalent

*E-mail: mouradef@natur.cuni.cz

homogeneous half-space introduced by Gomez-Trevino (1987).

McNeill (1980) described the basic principles of the EMI method using electromagnetic dipoles with fixed source–receiver distance in the frequency domain and the concept of the relative and cumulative response functions. These functions have been widely used as a powerful tool for forward modelling and interpretation of measurements obtained by conductivity meters operating at LINs for 1D layered earth models. Monteiro Santos (2004) used these functions to perform 1D laterally constrained inversion of EMI data in two freeware inversion software packages: *EM-34-2D* and *EM34-3D*. Loke (2006) also used them in his freely available EMI 1D modelling and inversion software *FreqEM*. These well-known functions were derived and should be used for the instruments laid on the surface of the earth. In the present paper, we propose new generalised relative and cumulative response functions, which can be used for instruments operating at any height from the surface and perform quantitative analyses of the behaviour of the relative response function and the depth of investigation of EMI instruments, when raised from the ground.

THEORY

Let us consider a homogeneous half-space on the surface of which an electromagnetic induction (EMI) equipment is located. We can consider that the half-space is formed by an infinite number of thin layers of thickness dz at depth z (here, z denotes the depth of the thin layer normalised by the inter-coil distance s). It is possible to calculate the secondary magnetic field in the receiver coil arising from the current flowing within any of these thin layers. Using the low induction number approximation, McNeill (1980) constructed a function, $\Phi_V(z)$, for the vertical dipole coil configuration as follows:

$$\Phi_V(z) = \frac{4z}{(4z^2+1)^{3/2}}, \tag{1}$$

which describes the relative contribution of the secondary magnetic field arising from a thin layer at any depth z to the total secondary magnetic field in the receiver coil. Differentiating equation (1) with respect to z and setting it equal to 0, we see that the material located at a depth of $z = \sqrt{1/8}$ gives the maximum contribution to the secondary magnetic field. It is interesting to note that the near-surface material (z close to 0) gives a very small contribution to the secondary magnetic field, and therefore, this coil configuration is quite insensitive to changes in near-surface conductivity.

For the case of the horizontal dipole (VCP) configuration, the function $\Phi_H(z)$ is as follows:

$$\Phi_H(z) = 2 - \frac{4z}{(4z^2+1)^{1/2}}. \tag{2}$$

Here, the relative contribution from the near-surface material ($z = 0$) is maximum, and the response falls off monotonically with depth.

According to McNeill (1980), the construction of these response functions is possible because, when using the low induction number (LIN) approximation, one can assume that "(i) all current flow is horizontal and (ii) all current loops are independent of all other current loops". As the definition of apparent conductivity, using the LIN approximation, is given in terms of the secondary magnetic field at the receiver, we can see that the functions Φ also give the relative contribution from material at different depths to the apparent conductivity read by the EMI instrument. The integrals of functions (1) and (2) from zero to infinity give the total secondary magnetic field at the receiver coil from the entire half-space (note that as functions $\Phi_{V|H}$ are relative, the integrals $\int_0^\infty \Phi_{V|H}(z)\,dz = 1$), which is directly related to the electrical conductivity of the half-space. It is therefore possible to derive with great precision the relative influence of material at different depths to the measured apparent conductivity when operating at LINs.

The functions Φ shown above are useful to describe the relative sensitivity of the two coil configurations to material at various depths. However, McNeill (1980) described a function that is more useful for performing calculations. It is defined as the relative contribution to the secondary magnetic field, or to the apparent conductivity, from all material below an assigned depth z and is given as follows:

$$R_{V|H}(z) = \int_z^\infty \Phi_{V|H}(z)\,dz. \tag{3}$$

It is called the cumulative response function and can be written for vertical and horizontal dipole in the vertical coplanar (VCP) configurations as follows:

$$R_V(z) = \frac{1}{(4z^2+1)^{1/2}} \tag{4}$$

and

$$R_H(z) = (4z^2+1)^{1/2} - 2z. \tag{5}$$

Equation (4) shows, for example, that, for the vertical dipole configuration, all materials below a depth of approximately $1.94s$ yield a relative contribution of approximately 0.25 (i.e., 25%) to the secondary magnetic field at the receiver

coil. We can see from equation (5) that, for the horizontal dipole (VCP) case, the 25% contribution threshold is below a depth of 0.94*s*. Note that the above equations (1), (2), (4), and (5) were derived and are valid for the case where the instruments are laid on the surface of the ground.

METHODOLOGY AND EXAMPLES

In this paper, we calculated the functions Φ numerically by creating one-dimensional (1D) models consisting of a thin layer at depth z, with conductivity σ and thickness Δz surrounded by insulate material. We computed the off-phase component of the magnetic field using the full solution of Maxwell's equations for these 1D models and divided it by the off-phase component for the homogeneous medium with conductivity σ. Alternatively, we converted the off-phase components into apparent conductivities of these 1D models, using the methodology suggested by Andrade, Fischer and Valenta (2016), and divided it by the conductivity of the homogeneous medium σ.

The electromagnetic forward modelling solution, based on the full Maxwell's equations for vertical and horizontal dipole (VCP) source–receiver combinations with an inter-coil separation s over a 1D layered earth with N layers over an infinite half-space with conductivity σ_{N+1}, is given by Keller and Frischknecht (1966) and Anderson (1979) in terms of the mutual coupling ratio (Q), which is the ratio between the secondary and the primary magnetic field at the receiver coil as follows:

$$Q^V(s) = \frac{H^S}{H^P} = -s^3 \int_0^\infty R_0(\lambda) J_0(s\lambda) \lambda^2 e^{-2\lambda h} d\lambda \quad (6)$$

and

$$Q^H(s) = \frac{H^S}{H^P} = -s^2 \int_0^\infty R_0(\lambda) J_1(s\lambda) \lambda e^{-2\lambda h} d\lambda, \quad (7)$$

where J_0 and J_1 are the first kind zero-order and first-order Bessel functions, λ is the radial wave number, h is the height of the dipoles from the ground, and $R_0(\lambda)$ is called the reflection factor, which depends on the thicknesses and the electrical conductivities of each layer and is calculated at the interface between the air and the first layer. It can be obtained recursively beginning from the bottom layer N observing that there are no upcoming waves from the lower half-space, so $R_{N+1} = 0$ and the following:

$$R_n(\lambda) = \frac{(\Gamma_n - \Gamma_{n+1})/(\Gamma_n + \Gamma_{n+1}) + R_{n+1} e^{-2\Gamma_{n+1} d_{n+1}}}{1 + (\Gamma_n - \Gamma_{n+1})/(\Gamma_n + \Gamma_{n+1}) R_{n+1} e^{-2\Gamma_{n+1} d_{n+1}}}, \quad (8)$$

where $\Gamma_n = \sqrt{\lambda^2 + i\omega\mu_0\sigma_n}$, d_n and σ_n are the thickness and the electrical conductivity of the n^{th} layer, μ_0 is the permeability of vacuum, and ω is the angular frequency. $R_0(\lambda)$ is obtained assuming layer 0 as the air with $\sigma_0 = 0$. For a homogeneous earth case, we just have to consider the model as composed of one single infinity layer with the conductivity of the ground. The integrals in equations (6) and (7) and the Hankel transforms of functions $\lambda^2 R_0 e^{-2\lambda h}$ and $\lambda R_0 e^{-2\lambda h}$, respectively, can be calculated by linear filtering. Here, we used the Guptasarma and Singh (1997) filters with 120 elements for the Hankel J_0 transform and 140 elements for the Hankel J_1 transform.

In the methodology suggested by Andrade *et al.* (2016), equations (6), (7), and (8) are used to find a homogeneous ground conductivity value (σ) that leads to the same, or very similar, obtained values of the off-phase component of Q for the thin layer 1D model (apparent conductivity σ_a). In other words, this problem can be solved by finding the root (zero) of the function $g(\sigma) = (\Im(Q^{mod}) - \Im(Q^{hom}(\sigma)))$ by the Newton–Rhapson iterative method, where Q^{mod} is computed for the thin layer 1D model and $Q^{hom}(\sigma)$ is obtained assuming a homogeneous medium with conductivity σ. Starting from an initial guess (σ_0) of the apparent conductivity, obtained by the low induction number approximation equation as follows:

$$\sigma_a = 4\frac{\Im(Q)}{\omega\mu_o s^2}, \quad (9)$$

the iterative method finds successively better estimations of σ until a sufficiently close-to-zero value of $g(\sigma)$ is reached.

We tested both methods (off-phase ratio and apparent conductivity ratio), assuming $h = 0$, for the technical specifications of several known brands of conductivity meters (*Geonics EM-31* and *EM-34*, *GF Instruments CMD-Explorer* and *CMD-MiniExplorer*). Very good agreements between both methods and equations (1) and (2) were found even for conductivities up to 0.5 S/m, meaning that it is possible to use equations (1) and (2) for these instruments with a very good accuracy if one assumes the low induction number approximation. Negligible differences were observed between the values of Φ obtained by equations (1) and (2) and by the numerical method for the *Geonics EM-34* specifications (Fig. 1), only at higher conductivities (blue curve). We want to emphasise that it does not mean that the low induction number approximation equation (9) for obtaining the apparent conductivity is valid up to very high conductivity values but only that the relative and cumulative response equations are valid for the tested equipments even at such high conductivities as the assumption that all current loops within a infinitesimal

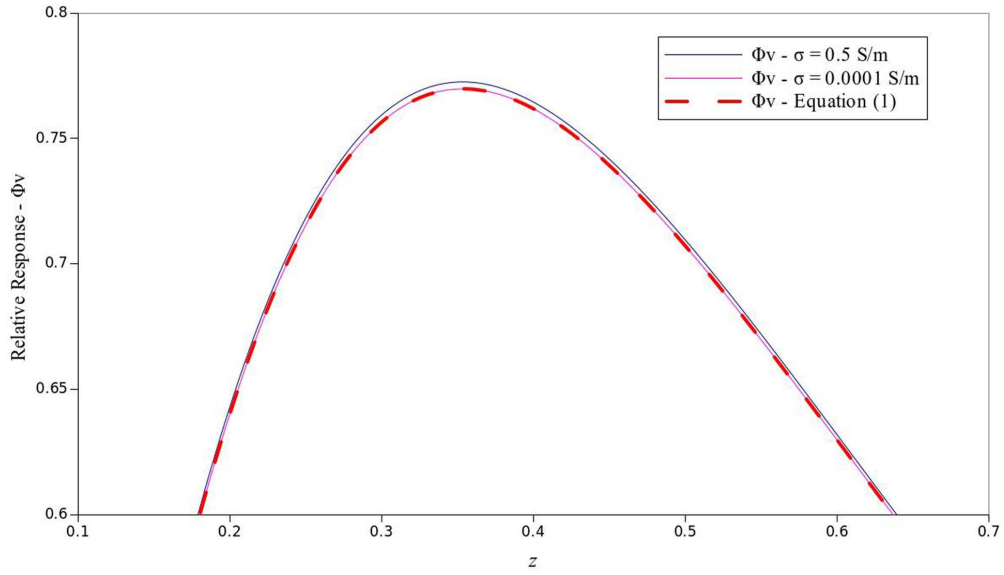

Figure 1 Relative response function $\Phi_V(z)$ for the *EM-34* specifications calculated by equation (1) and numerically for two extreme values of conductivities.

thin layer are independent of all other current loops is valid at low induction numbers and that, over either a homogeneous or horizontally stratified earth, all current flow is horizontal so that no current crosses the interfaces. Andrade *et al.* 2016 made a detailed study of the errors observed when using the low induction number equation (9) for several well-known brands of conductivity meters and found that errors greater than 5% can be found even at conductivities of 10 mS/m.

To obtain generalised relative and cumulative response functions for the case of the instrument being operated at some height (h) from the surface of the ground, we again used equations (6), (7), and (8). As an example, Fig. 2 shows the results for the numerically calculated relative response functions for the vertical dipole, using the specifications of the *GF Instruments CMD-Explorer* with $s = 4.49$ m, with the instrument used at 1 m above the ground ($h = 1$ m), for half-space conductivities of 0.5 and 0.001 S/m along with the plot of the relative response at the surface ($h = 0$) obtained by equation (1). We can see that the numerically obtained functions are quite the same for both conductivities. It is also found that these numerical functions for the instrument at $h = 1$ m from the ground are almost entirely equal to the analytical expressions from equation (1) ($h = 0$) shifted to the left along the horizontal axis (in the *z-axis* direction) and scaled by a constant factor F along the vertical axis (relative response axis). It is obvious to deduce that the shift in the *z-axis* direction is equal to the height (h) of the equipment from the ground (normalised by s), as the instrument, when raised from the ground, is *shifted* by h in the opposite direction of the *z-axis*.

To obtain the scale factor F, let us denote the blue hatched area as A_1, which by definition must be equal to 1 (note that, in Fig. 2, the functions are only plotted up to $z = 2$, but $A_1 = 1$ for $z \to \infty$ as $A_1 = \int_0^\infty \Phi_V(z)\, dz = 1$), and the pink area as A, which is also by definition $A = \int_{h/s}^\infty \Phi_V(z)\, dz = R_V(h/s)$ given by equation (4). As noted before, analysing the curves in Fig. 2, the relative response values for $h = 1$ m are equal to the relative response values for $h = 0$ m, shifted to the left in the *z-axis* direction by h/s and multiplied by a factor F in such a way that these two areas are also related by the factor F so that we can write $A_1 = AF \to R_V(h/s)\, F = 1$, and finally, we obtain $F = 1/R_V(h/s)$. It can be shown that this is also valid for the horizontal dipole (VCP) configuration, so one can obtain expressions for the scaling factors for both vertical (F_V) and horizontal (F_H) dipole configurations from equations (4) and (5) as follows:

$$F_V = [4(h/s)^2 + 1]^{1/2} \tag{10}$$

and

$$F_H = \frac{1}{[4(h/s)^2 + 1]^{1/2} - 2(h/s)}. \tag{11}$$

Therefore, if the equipment is measuring at some height, h, from the surface, the generalised relative response functions can be obtained by adding the shift (h/s) to z in equations (1)

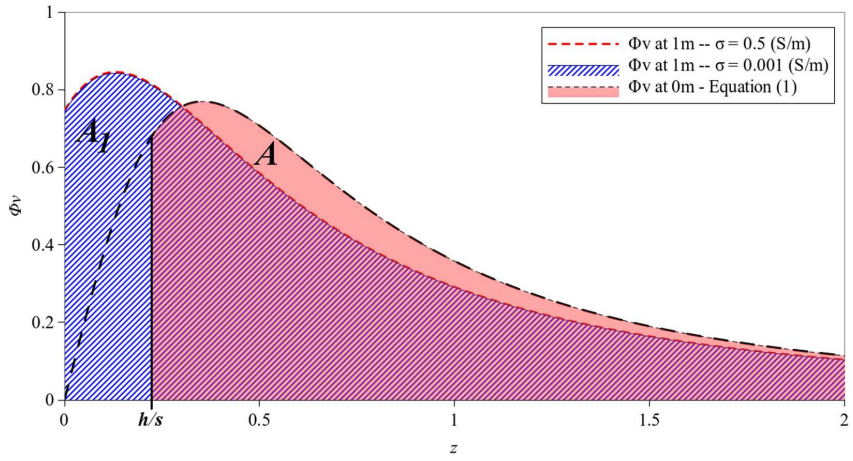

Figure 2 Relative response function $\Phi_V(z)$ according to equation (1) and numerically calculated for the *CMD-Explorer* specifications ($s = 4.49$ m) at 1 m from the ground and two different conductivities.

and (2) and multiplying them by the scaling factors (10) and (11), respectively, as follows:

$$\Phi_V(z,h,s) = [4(h/s)^2+1]^{1/2}\frac{4(z+h/s)}{[4(z+h/s)^2+1]^{3/2}} \tag{12}$$

and

$$\Phi_H(z,h,s) = \left(2 - \frac{4(z+h/s)}{[4(z+h/s)^2+1]^{1/2}}\right) \times \frac{1}{[4(h/s)^2+1]^{1/2} - 2(h/s)}. \tag{13}$$

In the same way as above, differentiating equation (12) with respect to z and setting it equal to 0, we see that the material located at a depth of $z = \sqrt{1/8} - h/s$ gives the maximum contribution to the secondary magnetic field for the generalised case. It is clear that when $h/s > \sqrt{1/8}$, the maximum contribution comes from zero depth, $z = 0$.

In Fig. 3, we show, as examples, the functions $\Phi_V(z,h,s)$ and $\Phi_H(z,h,s)$ for all the *CMD-Explorer* possible configurations operated at 1 m from the ground. For the sake of comparison, we have also plotted the curve for $h = 0$. It is interesting to note that, based on the analysis of the $\Phi_V(z,h,s)$ function (12) and Fig. 3, when using the equipment at some height h from the ground, the influence of the near-surface material ($z = 0$) increases as the ratio (h/s) increases up to $h/s = 0.5$. Then, it decreases for larger values of this ratio when the curves behave very similarly as the relative response function for the horizontal (VCP) dipole configuration. In other words, if we have an equipment with inter-coil distance s and we raise it from the ground to some height h, the influence of the near-surface material increases up to the value of h equal to the half of s, and then, this influence starts to decrease as we further increase h. To arrive to this threshold of $h/s = 0.5$, we just had to set $z = 0$ in equation (12) and set the derivative with respect to the ratio (h/s) to 0 as follows:

$$\Phi_V(z=0,h,s) = \frac{4(h/s)}{4(h/s)^2+1} \Rightarrow \frac{d\Phi_V(z=0,h,s)}{d(h/s)} = 0 \rightarrow 4\left(\frac{h}{s}\right)^2 + 1 = 8\left(\frac{h}{s}\right)^2 \rightarrow \frac{h}{s} = \frac{1}{2}. \tag{14}$$

The initial increase of the relative response function for the vertical dipole case at $z = 0$ when elevating the instrument was already mentioned by McNeill (1980). Here, we quantified this effect using the generalised relative response curves. It can be also seen from equation (12) that the maximum value of Φ_V is 1 for $h/s = 0.5$ at $z = 0$.

Integrating equations (12) and (13) using equation (3), we obtain the cumulative response functions for the generalised case. It occurs that they are also shifted and scaled in the same way as the relative response functions and are given as follows:

$$R_V(z,h,s) = \frac{[4(h/s)^2+1]^{1/2}}{[4(z+h/s)^2+1]^{1/2}} \tag{15}$$

and

$$R_H(z,h,s) = \frac{[4(z+h/s)^2+1]^{1/2} - 2(z+h/s)}{[4(h/s)^2+1]^{1/2} - 2h/s}. \tag{16}$$

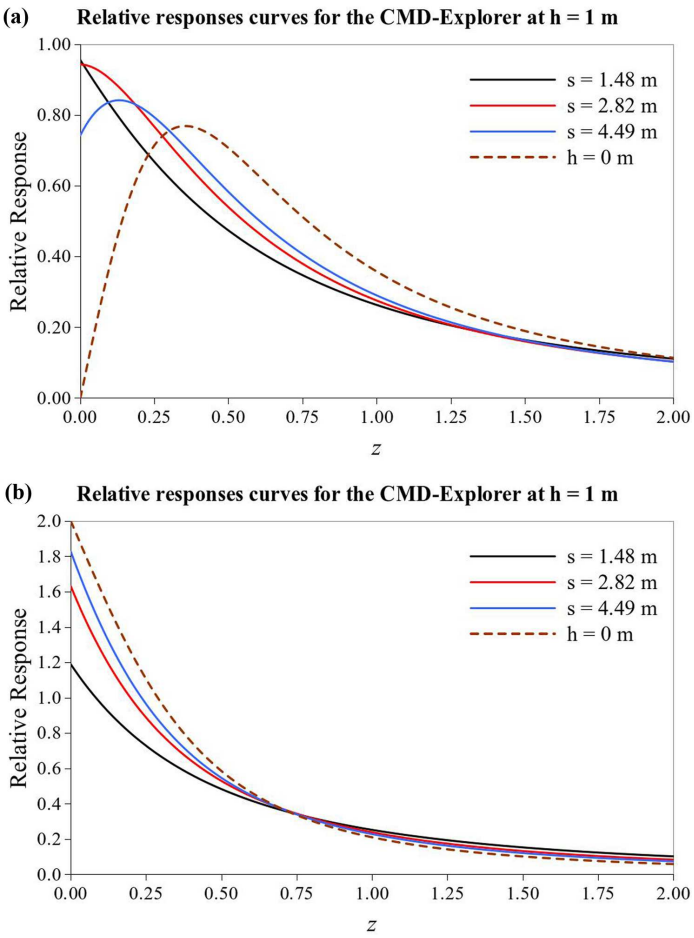

Figure 3 Relative response curves for all possible *CMD-Explorer* configurations at $h = 1$ m from the ground and for $h = 0$, for **a**) vertical and **b**) horizontal (VCP) dipoles.

Linear regressions between the numerically obtained response functions and the algebraic expressions in equations (12), (13), (15), and (16) show almost perfect agreement with coefficients of determination (R^2) and slope terms equal to 1 and intercept terms equal to 0 up to the sixth decimal place for all the studied instrument specifications and conductivities smaller than 0.5 S/m.

In Fig. 4, we show the functions $R_V(z,h,s)$ and $R_H(z,h,s)$ for all possible *CMD-Explorer* configurations operated at $h = 1$ m from the ground. For the sake of comparison, the curve for $h = 0$ is plotted as well.

DISCUSSION

According to Spies (1989), Frischknecht *et al.* (1989) and McNeill (1980), the depth of investigation (DOI) of electromagnetic induction equipment operating at very low induction numbers, when the penetration of the electromagnetic fields is not limited by the skin depth effect, depends mainly on the inter-coil distance s and on the dipole orientation. It is usually associated to a depth that corresponds to a preselected percentage (70% or 80%) of the total response from the material above it and corresponds to some value of $R_{V|H}$. For example, if setting $R_{V|H} = 0.3$ and $h = 0$ one can obtain, algebraically or numerically from equations (15) and (16), the value of z, defined as the DOI, which is equal to $1.59s$ for the vertical dipole mode and $0.76s$ for the horizontal dipole (VCP) (70% of the relative contribution to the apparent conductivity is coming from the material above the DOI). We can see that the above-obtained values corresponding to $R_{V|H} = 0.3$ are very similar to the well-known rule of thumb for the DOIs of $1.5s$ and $0.75s$ for the vertical and horizontal (VCP) dipole configurations.

Looking at Fig. 4, one can see that the DOI for the horizontal dipole (VCP) mode increases with the increasing height of the instrument. For the vertical dipole mode, the DOI first

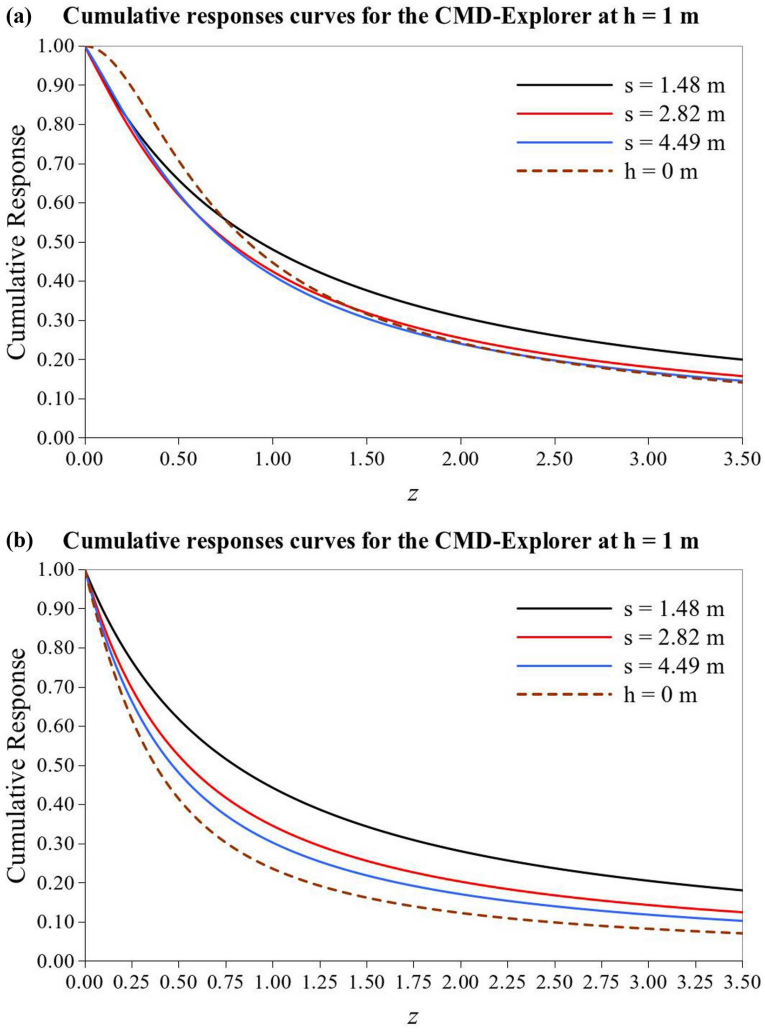

Figure 4 Cumulative response curves for all possible *CMD-Explorer* configurations at $h = 1$ m from the ground and for $h = 0$, for **a**) vertical and **b**) horizontal (VCP) dipoles.

decreases and then increases. This effect was already noted by McNeill (1980) and Interpex Limited (2008). We can explain and quantify this behaviour for the vertical dipole mode in the following way: the DOI, as defined above, normalised by s, can be obtained for the vertical dipole configuration, making $z = DOI$ in equation (15) for a chosen value of R_V, as follows:

$$DOI = \frac{\sqrt{4(h/s)^2 + 1 - R_V^2}}{2R_V} - \frac{h}{s}. \tag{17}$$

We can see that this equation decreases and then increases with increasing values of h/s. Differentiating equation (17) with respect to (h/s) and setting it equal to 0 as follows:

$$\frac{dDOI}{d(h/s)} = \frac{2\,h/s\,[4(h/s)^2 + 1 - R_V^2]^{-1/2}}{R_V} - 1 = 0$$
$$\rightarrow \frac{2h/s}{\sqrt{4(h/s)^2 + 1 - R_V^2}} = R_V \rightarrow \frac{h}{s} = \frac{R_V}{2}, \tag{18}$$

we see that the DOI for the vertical dipole has a minimum value at $h/s = R_V/2$, in other words, depending on the value of R_V chosen to define the DOI, when one raises the equipment from the ground, the DOI decreases up to a height equal to $sR_V/2$, and after that height, the DOI starts to increase. It turns out from equations (17) and (18), for example, that the minimum value of the DOI for the vertical dipole case is $1.52s$ at $h = 0.15s$ for $R_V = 0.3$. Comparing this result with

the result for $h = 0$ shown above, we see that, for the vertical dipole case, this initial decrease in the DOI with increasing h is not very significant.

Again, the behaviour of the DOI for the vertical dipole mode when elevating the instrument was already mentioned by McNeil (1980) in a qualitative way, and here, it is shown how to evaluate it algebraically.

CONCLUSION

We have shown that the well-known relative and cumulative response equations for electromagnetic induction (EMI) instruments operated on the earth surface can be used for several brands of conductivity meters operating at low induction numbers as they show very good agreements with numerically calculated response functions by the full solution of Maxwell's equations.

We have obtained generalised analytical expressions for the relative and cumulative response functions for the case when the instruments are operated at any height from the ground, which also showed almost exact agreements with the numerically calculated response functions for instruments operating at low induction numbers.

Analysing the obtained generalised equations, we have shown that when an EMI equipment operating in the vertical dipole mode is raised by some height, h, above the ground, the influence of near-surface material increases until the height, h, equals the half of the inter-coil distance, s, and then, this influence starts to decrease for larger values of h. We have also seen that the depth of investigation for the vertical dipole mode also varies with height: it decreases until the height, h, equals the half of the inter-coil distance, s, multiplied by the value of the cumulative response function used to define it, and then increases with increasing h.

ACKNOWLEDGEMENT

The authors would like to thank the Fundação Cearense de Meteorologia e Recursos Hídricos and the government of the State of Ceará, Brazil, for granting the first named author license to undertake his doctoral studies in Prague.

REFERENCES

Anderson W.L. 1979. Numerical-integration of related Hankel transforms of orders 0 and 1 by adaptive digital filtering. *Geophysics* **44**(7), 1287–1305.

Andrade F.C.M., Fischer T. and Valenta J. 2016. Study of errors in conductivity meters using the low induction number approximation and how to overcome them. *Near Surface Geoscience*, Barcelona, Spain, Extended Abstracts. European Association of Geoscientists and Engineers.

Babacan A.E., Sahin A.B. and Cinar U. 2016. The investigation of seawater intrusions with electric and electromagnetic methods—A case study from eastern Black Sea. *Near Surface Geoscience*, Barcelona, Spain, Extended Abstracts. European Association of Geoscientists and Engineers.

Callegary J.B., Ferré T.P.A. and Groom R.W. 2007. Vertical spatial sensitivity and exploration depth of low-induction-number electromagnetic-induction instruments. *Vadose Zone Journal* **6**(1), 158–167.

Frischknecht F.C., Labson V.F., Spies B.R. and Anderson W.L. 1989. Profiling methods using small sources penetration. In: *Electromagnetic Methods in Applied Geophysics*, Vol. **2**, part A (ed M.N. Nabighian), pp. 105–270. Society of Exploration Geophysicists.

Gomez-Trevino E. 1987. Nonlinear integral equations for electromagnetic inverse problems. *Geophysics* **52**(9), 1297–1302.

Guillemoteau J., Sailhac P., Boulanger C. and Trules J. 2015. Inversion of ground constant offset loop-loop electromagnetic data for a large range of induction numbers. *Geophysics* **80**(1), E11–E21.

Guptasarma D. and Singh B. 1997. New digital linear filters for Hankel J_0 and J_1 transforms. *Geophysical Prospecting* **45**, 745–762.

Hulin G., Maneuvrier C., Vincent J.B. and Tabbagh A. 2015. What exists beneath the place where Conrad Schlumberger achieved the first (1912) electrical prospection experiment. *Near Surface Geoscience*, Turin, Italy, Extended Abstracts. European Association of Geoscientists and Engineers.

Interpex Limited 2008. *IX1D v3 Instruction Manual*, Version 1.11. Interpex Limited, Golden, CO, 133 pages.

Keller G. and Frischknecht F.C. 1966. Electrical methods in geophysical prospecting. *International series of monographs in electromagnetic waves 10*. Pergamon Press, Oxford, New York.

Loke M.H. 2006. FreqEM - 1-D frequency domain EM modelling. *Pug Soft Inc*. Online available at http://www.geotomosoft.com/downloads.php.

Martini E., Werban U., Wollschläger U., Pohle M., Dietrich P. and Zacharias S. 2015. On the use of repeated EMI measurements for mapping soil moisture and implications for soil mapping. *Near Surface Geoscience*, Turin, Italy, Extended Abstracts. European Association of Geoscientists and Engineers.

McNeill J.D. 1980. Electromagnetic terrain conductivity measurement at low induction numbers. *Geonics Limited Technical Note TN-6*, Ontario.

Monteiro Santos F.A. 2004. 1-D laterally constrained inversion of EM34 profiling data. *Journal of Applied Geophysics* **56**, 123–134.

Spies B.R. 1989. Depth of investigation in electromagnetic sounding methods. *Geophysics* **54**(7), 872–888.

Appendix C

Quick Inversion of Multi-configuration Electromagnetic Induction Data Using Cumulative Response Functions

F.C.M. Andrade and T. Fischer

23rd European Meeting of Environmental and Engineering Geophysics

EAGE - Near Surface Geoscience, Malmö, Sweden, Extended Abstracts. 2017

DOI: 10.3997/2214-4609.201702119

We 23P2 18

Quick Inversion of Multi-configuration Electromagnetic Induction Data Using Cumulative Response Functions

F.C.M. Andrade* (Charles University in Prague), T. Fischer (Charles University in Prague)

Summary

In this paper we present a quick method for one-dimensional inversion of multi-configuration electromagnetic induction data, obtained by instruments operating at low induction numbers, using cumulative response curves. As it is very fast and easily programmed it can be used when a real-time quick inversion in the field is desired and as a good initial guess model estimation for more sophisticated inversion techniques. In the proposed technique we make use of several measurements of apparent conductivity, performed with different transmitter-receiver dipoles configurations in a same location to estimate a one-dimensional model where the number of layers is equal to the number of measurements. The depths of the bottom of the layers are estimated as the depths of investigation of each configuration measurement. The conductivities of the first two layers are obtained by solving the linear system formed by the forward modelling equations for computing the apparent conductivity using the cumulative response functions for the two first configurations measurements. The conductivities of the remaining layers are obtained recursively using the previous estimated conductivities and the data measured by the following configurations using the same approach.

Introduction

Inversion of geophysical data is one of the greatest problems in applied geophysics as they are in general under-determined and the data is contaminated by noise and thus may have a huge number of solutions which would lead to a good fit between observed and modelled data. Geoelectric and electromagnetic induction (EMI) methods are also very much affected by these problems because of, for example, the principle of equivalence in one-dimensional (1-D) models. For a good inversion result, geophysicists must also take into account geology, in the form of a-priori information, when one can take into account in the misfit function to be optimized the deviations from the a-priori model parameters. These a-priori model space parameters can be obtained either by geological maps, samples from boreholes, geophysical data from another method, well-logging data and so on. In many situations when these information are not available, like when a real-time quick inversion in the field is desired, or when wanting to obtain a first guess model for initiating more sophisticated inversion techniques, a fast and accurate inversion technique which uses only the observed data as input can be very useful.

In this paper we present a quick multi-configuration EMI data 1-D inversion technique using cumulative response functions for instruments operating at low induction numbers. In the proposed technique we make use of several measurements of apparent conductivity, performed with different transmitter-receiver dipoles configurations in a same location, to estimate a 1-D model where the number of layers is equal to the number of measurements. The configurations parameters that may vary are the inter-coil distance, the dipoles orientation (vertical or horizontal) and the height of the instrument from the ground.

Theory

McNeill (1980) calculated the apparent conductivity (σ_a) of a 1-D layered earth with N layers over an infinite half-space with conductivity σ_{N+1}, measured by an EMI instrument operating at low induction numbers with inter-coil distance (s) using the cumulative response functions which is defined as the relative contribution to the secondary magnetic field or apparent conductivity from all material below a given depth z. We can prove that the generalized forms of these well-known functions for the instrument at any height h from the ground are given as:

$$R_V(z,h,s)=\frac{[4(h/s)^2+1]^{1/2}}{[4(z+h/s)^2+1]^{1/2}} \quad \text{and} \quad R_H(z,h,s)=\frac{[4(z+h/s)^2+1]^{1/2}-2(z+h/s)}{[(4(h/s)^2+1)]^{1/2}-2h/s}, \tag{1}$$

where R_V and R_H are the cumulative response functions for the vertical and horizontal dipoles configurations respectively. Here z is the depth normalized by the inter-coil distance s.

The apparent conductivity (σ_a) for a 1-D layered earth, for a given j configuration with inter-coil distance s_j and height from the ground h_j, is given by the sum over the product of the layer's conductivities and the difference of the cumulative response functions at the top and the bottom of each layer. It can be written in a compact form as:

$$\sigma_{aj}=\sum_{i=0}^{N}\sigma_{i+1}\left[R_{V/H}(z_i,h_j,s_j)-R_{V/H}(z_{i+1},h_j,s_j)\right] \tag{2}$$

where z_i is the depth of the bottom of the layer i. Note that z_0=0 which leads to $R_{V/H}(z_0,h_j,s_j)$ = 1 and $R_{V/H}(z_{N+1},h_j,s_j)$ =0, as z_{N+1} is infinity.

As soon as we can make several measurements with different dipole configurations we can obtain several values of apparent conductivity in one spot and thus with NR measurements is therefore possible to invert the conductivities of a NR layered earth model.

Methodology

The first step is to estimate the depths of the bottom of the layers as the values of the depths of investigation of each configuration measurement. According to Spies (1989) and McNeill (1980) the

depth of investigation of EMI equipment operating at very low induction numbers, when the penetration of the electromagnetic fields is not limited by the skin depth effect, depends mainly on the inter-coil distance *s*, on the dipole orientation and the height *h* of the instrument from the ground. It is usually associated to a depth that corresponds to a preselected percentage (70% to 80%) of the total response from the material above it and corresponds to some value of $R_{V|H}$ (0.2 - 0.3). For example, if setting $R_{V|H}$ = 0.3 and h=0 one can obtain, algebraically or numerically from equations (1), the value of z, defined as the depth of investigation, which is equal to 1.59s for the vertical dipole mode and 0.76s for the horizontal dipole. These values are very similar to the well-known rule of thumb for the depth of investigations of 1.5s and 0.75s for the vertical and horizontal dipoles configurations.

The second step is to sort the available measurements in ascending order of the depth of investigation of their configuration. The depth of investigation (*DOI*) as defined above can be obtained for the vertical dipole configuration from equation (1) for a chosen value of R_V as:

$$DOI = \frac{s\sqrt{4(h/s)^2+1-R_V^2}}{2R_V} - h \quad . \tag{3}$$

For the horizontal dipole configuration the depth of investigation can be obtained numerically solving equation (1) for the value of z that makes the equation equals the chosen value of R_H.

The third step is to calculate the conductivities of the *NR* layers. To obtain the conductivities of the first two layers we use equation (2) for the first two configurations, assuming a two layered earth model, to create a two equation linear system, which can be written as:

$$\sigma_{a1} = \sigma_1\left[1 - R_{V|H}(z_1, h_1, s_1)\right] + \sigma_2 R_{V|H}(z_1, h_1, s_1) \quad \text{and} \tag{4}$$

$$\sigma_{a2} = \sigma_1\left[1 - R_{V|H}(z_1, h_2, s_2)\right] + \sigma_2 R_{V|H}(z_1, h_2, s_2) \quad , \tag{5}$$

so that we can obtain σ_1 and σ_2 from (4) and (5) as:

$$\sigma_1 = \frac{\sigma_{a1} R_{V|H}(z_1, h_2, s_2) - \sigma_{a2} R_{V|H}(z_1, h_1, s_1)}{R_{V|H}(z_1, h_2, s_2) - R_{V|H}(z_1, h_1, s_1)} \quad \text{and} \quad \sigma_2 = \frac{\sigma_{a2} - \sigma_1\left[1 - R_{V|H}(z_1, h_2, s_2)\right]}{R_{V|H}(z_1, h_2, s_2)} \quad . \tag{6}$$

With the previous obtained values of σ_1 and σ_2 we can estimate the conductivity of the third layer (σ_3) using the value of apparent conductivity obtained with the third configuration (σ_{a3}). Developing equation (2) assuming a three layered earth model (we will omit the height parameter):

$$\sigma_{a3} = \sigma_1\left[1 - R_{V|H}(z_1, s_3)\right] + \sigma_2\left[R_{V|H}(z_1, s_3) - R_{V|H}(z_2, s_3)\right] + \sigma_3 R_{V|H}(z_2, s_3) \quad , \tag{7}$$

we can see that is straight forward to obtain σ_3. In the same way we can recursively obtain expressions to estimate the conductivities of the other layers with measurements from different configurations and the previous obtained conductivities as:

$$\sigma_j = \frac{\sigma_{aj} - \sum_{i=0}^{j-2} \sigma_{i+1}\left[R_{V|H}(z_i, h_j, s_j) - R_{V|H}(z_{i+1}, h_j, s_j)\right]}{R_{V|H}(z_{j-1}, h_j, s_j)} \tag{8}$$

We can see that the method can lead to negative values of conductivities depending on the calculated values of $R_{V/H}$ which depend on the values of the estimated depths of the bottom of the layers (z_i) which, by its turn, depend on the value of $R_{V/H}$ chosen to define the depth of investigation but it can always be avoided by changing the selected value of $R_{V/H}$.

To obtain the final results we make a direct search (repeating steps 1 to 3) within the values of $R_{V/H}$ used to define the depth of investigation and pick up the one that doesn't lead to negative values of conductivities and that minimizes the L1-Norm between the observed and calculated values of apparent conductivity by equation (2) using the model parameters obtained in the third step. Here the direct search was made within the range of $R_{V/H}$ from 0.15 to 0.35.

Examples

In the first example we used a synthetic model consisting of a 4-layered earth with conductivities of 50, 1, 10 and 0.5 mS/m and thicknesses of 3.5, 1.5 and 3.5 m. We used all six possible coil

configurations of *GF Instruments CMD-Explorer* (s=1.48, 2.82 and 4.49m in vertical and horizontal dipoles modes) at h=0 to compute the apparent conductivities and the depths of investigation. The value of $R_{V/H}$ which lead to the minimum L1-Norm misfit was found as 0.15. In Figure 1 we show the results of the methodology where the parameters of a 6 layered earth were estimated together with the apparent conductivities calculated by equation (2) for the inverted model and of the synthetic model. The apparent conductivities are plotted at the calculated depths of investigation. We can see that there's an almost perfect agreement in the apparent conductivities and that the inverted model agrees well in the top with the synthetic model and in the bottom it tends to overestimate a little the values of conductivity, not distinguishing well the third layer.

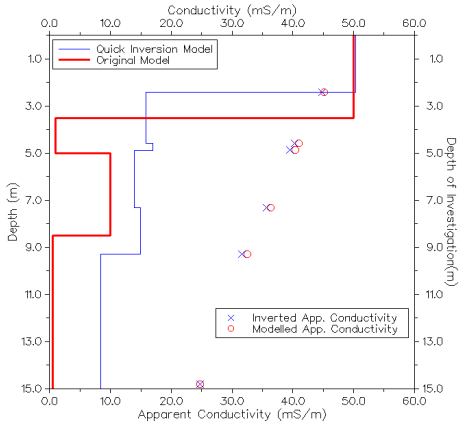

Figure 1 *Synthetic input model, the resultant model of the quick inversion methodology and the apparent conductivities calculated for both synthetic and inverted models of the first example.*

In the second example we show the results applied to real data. The data was collected in the Nová Ves kaolin mine near the town of Skalná, Czech Republic. The data was measured with 8 dipoles configurations using the *GF Instruments CMD-Explorer* and *Mini-Explorer* at h=0 and post-calibrated by a process similar to von Hebel et al. (2014). In the same location we've performed an ERT profile with a Wenner-Schlumberger array with minimum electrode distance of 1m. We used the freely available finite-difference based inversion software *DC2dInvRes* by Günther (2005) for inverting the ERT profile. We applied the quick inversion and the depths to the bottom of the layers were optimised by $R_{V/H}$ = 0.15. In Figure 2 a) we show the resultant inverted 8 layers model together with the results of the ERT data inversion for a 13 layers model and in b) the post-calibrated measured apparent conductivities and the calculated by equation (2) using the layered models parameters obtained by the quick inversion and by the ERT inversion. The labels on "Dipole configurations" axis are formed by the inter-coil distance (m) plus a code in which 0 stands for horizontal and 1 for vertical dipoles.

It is found that despite the differences between the models obtained by the EMI and ERT inversion there is a good agreement in the calculated apparent conductivities, which points to the non-unique character of the inverse problem. Interestingly, the agreement with the measured data is better for the quick inverted model than to the ERT inverted model. One must have in mind that the model obtained by ERT inversion is just another geophysical method data inversion and probably does not represent the true geology and that the ERT inversion algorithm searches for conductivities fixing the thicknesses of the layers by some criteria based on the dipole distances used in the measurements.

We can also see, from figures 1 and 2, that the values of the measured (synthetic) apparent conductivities approach the values of the apparent conductivities modelled using the inverted layers parameters with increasing depths of investigation and that they are the same for the greatest depth of investigation. To understand this behaviour we will discuss the case in which we constructed (inverted) a 3 layered model from three values of apparent conductivity σ_{a1}, σ_{a2} and σ_{a3} obtained by three different coil configurations. The apparent conductivity for the third configuration of such resultant model (σ'_{a3}) can then be written, using equation (2) and σ_3 from (7), as:

$$\sigma'_{a3}=\sigma_1\left[1-R_{V/H}(z_1,s_3)\right]+\sigma_2\left[R_{V/H}(z_1,s_3)-R_{V/H}(z_2,s_3)\right]+ \\ +\frac{\sigma_{a3}-\sigma_1\left[1-R_{V/H}(z_1,s_3)\right]-\sigma_2\left[R_{V/H}(z_1,s_3)-R_{V/H}(z_2,s_3)\right]}{R_{V/H}(z_2,s_3)}R_{V/H}(z_2,s_3) \rightarrow \sigma'_{a3}=\sigma_{a3} \quad (11)$$

In a similar way it can be proved for any number of layers.

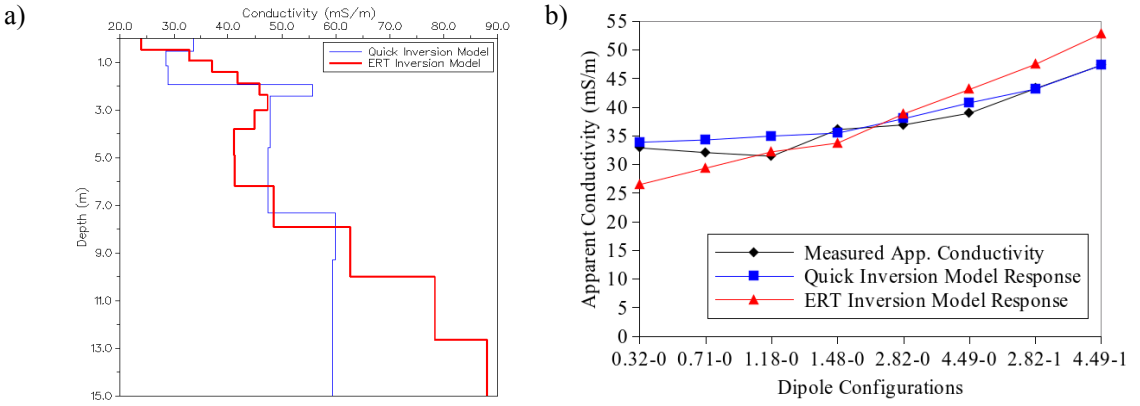

Figure 2 *a) The resultant model of the quick inversion methodology and the resultant model by ERT inversion from the data collected in the Nová Ves kaolin mine. b) Apparent conductivities calculated for both quick inverted and ERT inverted models and the data collected in the kaolin mine.*

Discussions and Conclusions

We have introduced a quick method for one-dimensional inversion of multi-configuration EMI data, obtained by instruments operating at low induction numbers, using cumulative response functions which leads to very good agreement between the measured (or synthetic) data and the forward modelling response of the inverted parameters. In the shown synthetic data example we could see that there was not a very good agreement between the synthetic model and the inverted model parameters due to the general inversion non-uniqueness problem, probably caused by the principle of equivalence. The same was observed in the field example when comparing the obtained inverted model parameters with the parameters obtained by inversion of ERT measurements, but we conclude that the results were good enough for a technique which does not include any a-priori information and therefore the presented quick inversion method can be very useful in the field, as it is fast and easy implemented, and to obtain an initial guess for a more sophisticated inversion technique. It is also possible to invert the thicknesses of the layers by some optimization method using the above described methodology to calculate the conductivities of the layers.

References

Günther, T. [2005] Inversion methods and resolution analysis for the 2D/3D reconstruction of resistivity structures from DC measurements, PhD Thesis, University of Mining and Technology, Freiberg.

McNeill, J.D. [1980] Electromagnetic terrain conductivity measurement at low induction numbers. *Geonics Limited Technical Note TN-6*, Ontario.

Spies, B. R. [1989] Depth of investigation in electromagnetic sounding methods. *Geophysics*, **54(**7), 872-888.

von Hebel, C., Rudolph, S., Mester, A., Huisman, J.A., Kumbhar, P., Vereecken, H. and van der Kruk, J. [2014] Three-dimensional imaging of subsurface structural patterns using quantitative large-scale multiconfiguration electromagnetic induction data, *Water Resources Research*, **50**, 2732–2748.

Appendix D

VLF Electromagnetic Data Inversion Starting from Current Density Pseudo-sections Obtained by Linear Filtering

F.C.M. Andrade and T. Fischer

21st European Meeting of Environmental and Engineering Geophysics

EAGE - Near Surface Geoscience, Turin, Italy, Extended Abstracts. 2015

DOI: 10.3997/2214-4609.201413816

NEAR SURFACE GEOSCIENCE 2015

We 21P1 08

VLF Electromagnetic Data Inversion Starting from Current Density Pseudo-sections Obtained by Linear Filtering

F.C.M. Andrade* (Charles University in Prague) & T. Fischer (Charles University in Prague)

SUMMARY

We used current density pseudo-sections obtained by linear filtering of VLF data to create a starting model for an inversion procedure using the Polak-Ribiere variant of the conjugate gradient method. The inversion procedure looks for the minimum error between the observed data and forward modelling data, obtained by a finite-difference algorithm, of the initial subsurface model, where the model parameters are changed iteratively. The inputs for the procedure are the host medium resistivity within a range given by the user, the number of cells that should be used as an approximation of the real medium and the desired accuracy. The lateral positions of the cells, forming the initial model, are obtained automatically by looking for zeros in the second derivative in descending parts of the observed data curves. The depths of the cells, as well as their resistivities, are obtained from the maximum values of the current density pseudo sections within a given range of cells centred in the previously obtained lateral positions. Results for two simple synthetic models are shown.

Introduction

The VLF (Very Low Frequency) electromagnetic geophysical method has been used during the last decades in mineral and groundwater prospecting and other hydrogeologic and environmental problems. In groundwater prospecting it is particularly suitable for locating saturated fracture zones in hard rocks. However, data interpretation is still in most cases been done in a qualitative way.

The nature of the VLF surveys, where the number of measured parameters is rather small and only a single frequency is used, makes the inversion of VLF data quite a difficult task. Karous and Hjelt (1983) developed a linear filter, which leads to current density pseudo-sections, that has been widely used for interpretation and gives a good general idea of the subsurface.

VLF forward modelling, the basic step for any inversion procedure, can be traced back to Kaikkonen (1977) who used the finite element technique. Ogilvy and Lee (1991) used the current density pseudo-sections and a forward modelling technique, proposed by Nissen (1986) using integral equations with simplified Green functions, to create a guide for interpreting various kinds of anomalies.

In this paper we used the Karous and Hjelt (1983) current density pseudo-sections to estimate an initial model of the subsurface and use an inversion procedure using the Polak-Ribiere variant of the conjugate gradient method which minimizes the error between the observed data and forward modelling data, obtained by a finite-difference algorithm.

Theoretical background and methodology

The VLF geophysical prospecting method uses powerful radio stations working in the frequency range from 15-30kHz as a source for the incident electromagnetic field. At sufficiently large distances from the transmitting antenna the primary field can be considered to be a plane wave. In a generic heterogeneous medium where an electromagnetic plane wave is propagating far from the source with a time harmonic dependency in the form e^{iwt} , the Maxwell Equations, that relates the electric and magnetic fields with the currents flowing in the medium for the quasi-stationary approximation are valid and can be written, together with the Ohm's Law, in the following form:

$$\nabla \times \vec{E} = -i\omega\mu\vec{H}, \quad (1)$$

$$\nabla \times \vec{H} = (\sigma + i\omega\epsilon)\vec{E} \quad (2)$$

where: $\vec{E}$ is the vector electric field, $\vec{H}$ is the vector magnetic field, ω is the angular frequency, given by $\omega = 2\pi f$ (f is the frequency in Hz), μ is the magnetic permeability, ε is the dielectric permittivity, i is the imaginary unit and σ is the electric conductivity.

Considering a two-dimensional medium with no variations in its physical properties along the y axis, all partial derivatives in relation to y are equal to zero. If we consider that the field experiments are taken in the direction perpendicular to the y axis, i.e., perpendicular to the structures which are in the direction of the VLF source, we get the E_x and H_y components equal to zero. Developing the curls in equations (1) and (2) and performing some differentiations and algebra we arrive at:

$$\frac{1}{i\omega\mu}\left(\frac{\partial^2 E_y}{\partial z^2}+\frac{\partial^2 E_y}{\partial x^2}\right)-(\sigma+i\omega\epsilon)E_y = 0. \quad (3)$$

In order to perform direct **VLF** modelling we just had to solve numerically equation (3) for E_y and then calculate the values of the H_z and H_x components by numeric differentiation. As the final result we calculate the real and imaginary parts of the ratio (H_z / H_x), which are the quantities measured by most of the **VLF** field equipments. We solved equation (3) by the finite differences method. To obtain the solution we divide the medium into square cells with M columns and N lines, and replace the partial derivatives in each cell (i , j) by a symmetric finite differences approximation. Using Δx as the size of the squares sides and defining $K_1=(i\omega\mu)^{-1}$ and $K_2= i\omega\varepsilon$, we finally obtain:

$$E_{i,j} = \frac{K_1\left(E_{i+1,j}+E_{i-1,j}+E_{i,j+1}+E_{i,j-1}\right)}{\left(\sigma_{i,j}+K_2\right)\Delta x^2+4K_1} \quad . \tag{4}$$

Considering the values of the electric field in the model boundaries as known and constants and applying equation (4) to all unknown values of the electric field, we can arrange the equations into a single matrix equation of the form $\vec{b}=A\vec{E}$ where $\vec{b}$ is a vector of known constants with *(M-2)*x*(N-2)* elements, $\vec{E}$ is a vector containing the unknown values of the electric field with the same number of elements and *A* is a *(M-2)*x*(N-2)* by *(M-2)*x*(N-2)* matrix of known coefficients. Performing matrix *A* inversion and then multiplying A^{-1} by $\vec{b}$ we can find the solution for the unknown values $E_{i,j}$. We can see that matrix *A* is sparse with only 5 non-zero diagonals so we used the Conjugate Gradient method for a sparse system as described by Press et al (1997) to invert it.

We used the following boundaries conditions:

- $E_{i,j} = 0$ for the last line of the grid, i.e., the inferior boundary of the model. We took the depth of this boundary as at least 2 times the value of the *skin depth* (δ), given by: $\delta = 503.3\sqrt{\rho_2 / f}$ where ρ_2 is the resistivity of the reference medium, i.e., the resistivity of the majority of the cells, excluding the anomalies and f is the frequency of the incident wave.
- $E_{i,j} = 1$ for the first line of the grid, i.e., the top boundary of the model inserted in the air. We took this altitude as at least two times the skin depth.
- For the lateral boundary conditions of the model, i.e., the values of the electric field for the first and for the last columns, we assume that the medium behaves like a 1-D model, i.e., the borders are far (at least 2.5 times δ) from any anomaly inside the reference medium. Therefore, we used the solution of an 1-D model in a similar way of the 2-D case, only that in this case matrix *A* is tridiagonal and we used a modified version of the Thomas algorithm also described in Press at al (1997) to invert it.

Inversion Procedure

For the inversion procedure we used the Polak-Ribiere variant of the conjugate gradient method, also described in Press at al (1997), which minimize the error between the observed data and the forward modelling data, obtained as described above. The procedure starts from an initial automatically guessed medium model with the exception of the host medium resistivity ρ_2. We used current density pseudo-sections obtained by linear filtering of VLF data introduced by Karous and Hjelt (1983) to obtain the initial model in the following way:

- By visual observation of the current density pseudo-sections (Figure 1b) obtained from the observed data (e.g. Figure 2) and taking into account the grid cell size (Δx) that will be used in the forward modelling, we choose the number of grid cells (n) that form the anomalies inside the host medium. The number n will influence the duration of the inversion procedure and its accuracy.
- The lateral position of the cells forming the initial model are obtained automatically looking for zeros in the second derivative in descending parts of the observed data curves. Thereafter, the algorithm picks the n maximum values of current density and their position in the pseudo-section within a given range of cells centred in the previously obtained lateral positions. The values of the resistivities of each n grid cells (ρ_i) are estimated by a power regression between the ratio (ρ_i/ρ_2) and the current density value j by the following equation: $\rho_i = 0.346\rho_2 j^{-1.375}$. This regression was obtained by performing several forward modellings of single cell models at different depths and with different (ρ_i/ρ_2) and calculating the maximum observed current density obtained for each forward modelling data. Note that this is just an initial guess for beginning the inversion procedure. As the estimated resistivity of each cell depends on ρ_2, we make an initial direct search for the optimum ρ_2 within a given range of values.
- It is known that the current density pseudo-sections tend to present maximum values shifted in depth with relation to the true anomalies and the dips of the anomalies may be only an approximate estimation (see Ogilvy and Lee (1991)). Before entering the inversion procedure the algorithm performs two separate direct searches: the first to optimize the depth of the whole block of cells and the second a lateral optimization of the position of individual cells. These procedures proved to decrease in a great amount the mean error between the observed (synthetic) and modelled data.

Thereafter, the algorithm enters the Polak-Ribiere variant of the conjugate gradient method to optimize the values of each cell's resistivity (ρ_i) as well the resistivity of the host medium (ρ_2).

Results

We tested the accuracy of our inversion procedure on two synthetic models. Our first example consists of a single dipping anomalous body with resistivity of 5 Ωm within a host medium with resistivity of 900 Ωm (Figure 1a), the frequency of the VLF transmitter is 16 kHz. The current density pseudo-section is shown in Figure 1.b. The resultant subsurface model from the inversion procedure without lateral optimization is shown in Figure 1c and with the lateral optimization in Figure 1.d. We used 18 cells as an initial guess and the resistivity of the host medium to be within the range from 700 to 1200 Ωm. We can see that the lateral optimization removed several cells from the initial guess which fits better the synthetic (observed) data, enhancing the position and the dip of the body.

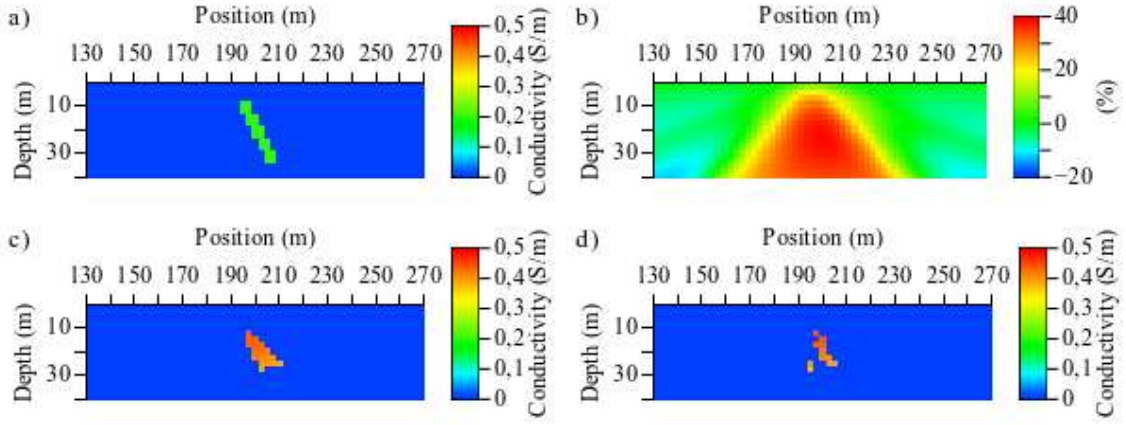

Figure 1 *a) The subsurface model used in example 1 with a dipping body within a host medium, b) The current density pseudo-section, c) The subsurface model resultant from the inversion procedure in example 1 without lateral optimization and d) with lateral optimization.*

The synthetic (observed) data and the inverted data with and without the lateral optimization (LO) are shown in Figure 2. We observed that the LO procedure decreased the average absolute error between the real part curves (synthetic and inverted) from 1.31 to 0.40.

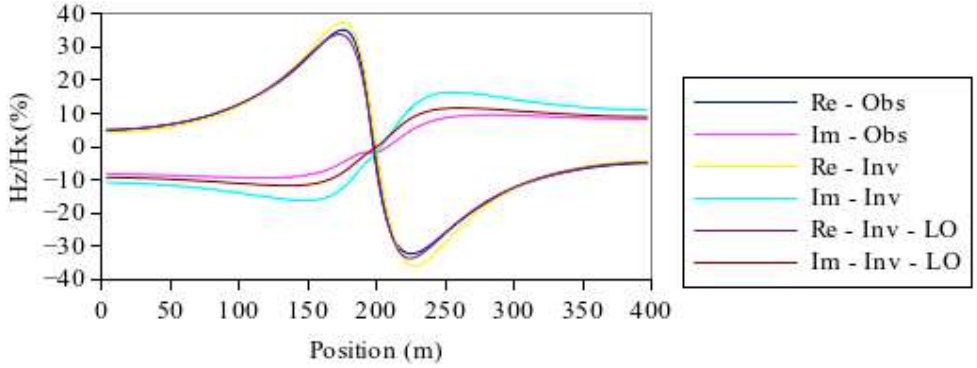

Figure 2 *The synthetic (observed) and inverted data from example 1.*

The second example consists of two vertical bodies with resistivities of 5 Ωm within a host medium with resistivity of 900 Ωm, the frequency of the VLF transmitter is 16 kHz. The model is shown in Figure 3a. The resultant subsurface model from the inversion procedure is shown in Figure 3b. We

used 24 cells as an initial guess and resistivity of the host medium to be within the range from 700 to 1200 Ωm. The synthetic (observed) data and the inverted data are presented in Figure 4. The average absolute error between the real part curves was of 0.41. We can see that, although the shapes of the bodies are not strictly correct, the inversion procedure was quite successful in determining their positions and resistivities.

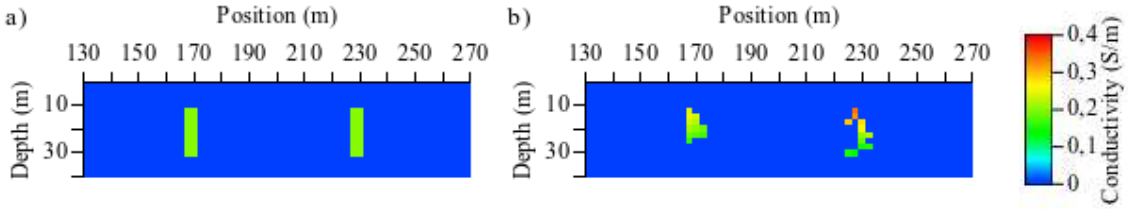

Figure 3 *a) The subsurface model used in example 2 with two vertical bodies, b) The model resultant from the inversion procedure in example 2.*

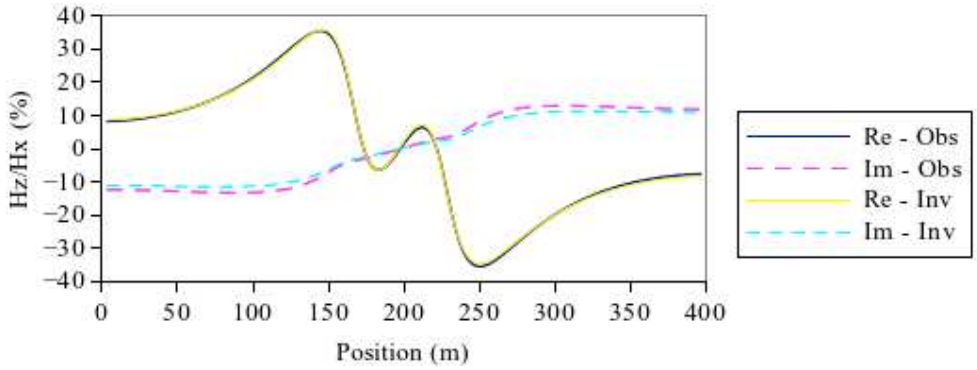

Figure *4 The synthetic (observed) and inverted data from example* 2.

Conclusions

The two examples succeeded in obtaining small differences between the synthetic and inverted curves and the inverted models showed that the methodology was quite good in positioning the anomalous bodies and gave a good indication of their dips and resistivities. The shapes of the inverted bodies were not in perfect agreement with the shapes of the subsurface model, which is probably caused by non-uniqueness of the inversion procedure, commonly present in geophysical methods.

References

Kaikkonen, P. [1977] A finite element program package for electromagnetic modelling. *Journal of Geophysics,* **43**, 179-192.

Nissen, J. [1986] A versatile electromagnetic modelling program for 2-D structures. *Geophysical Prospecting*, **34**(7), 1099-1110.

Karous, M. and Hjelt, S. E. [1983] Linear filtering of VLF dip-angle measurements. *Geophysical Prospecting*, **31**(5), 782-794.

Ogilvy, R. D. and Lee, A. C. [1991] Interpretation of VLF-EM in-phase data using current density pseudo-sections. *Geophysical Prospecting*, **39**(4), 567-580.

Press, W. H., Teukolsky, S. A., Vetterlin, W. T. and Flannery, B. P. [1997] *Numerical Recipes in Fortran 77: The Art of Scientific Computing (Vol. 1 of Fortran Numerical Recipes)*. Cambridge University Press, Cambridge.

Appendix E

Generalized Relative and Cumulative Response Functions for Conductivity Meters Operating at Low Induction Numbers

F.C.M. Andrade and T. Fischer

23rd European Meeting of Environmental and Engineering Geophysics

EAGE - Near Surface Geoscience, Malmö, Sweden, Extended Abstracts. 2017

DOI: 10.3997/2214-4609.201702034

Tu 23P1 09

Generalized Relative and Cumulative Response Functions for Conductivity Meters Operating at Low Induction Numbers

F.C.M. Andrade* (Charles University in Prague), T. Fischer (Charles University in Prague)

Summary

Relative and cumulative analytical response functions have been widely used as a powerful tool for forward modelling and interpretation of measurements obtained by electromagnetic induction conductivity meters operating at low induction numbers for one-dimensional layered earth models. These well-known functions were derived and should be used for the instruments laid on the surface of the earth. In this paper we extended these functions and obtained new generalized analytical expressions which can be used for instruments carried at any height from the surface. The proposed new equations were compared with numerically constructed functions, obtained using the full solution of the electromagnetic equations, and proved to be in very good agreement at low induction numbers.

Introduction

One of the most commonly used geophysical techniques for mapping the electrical conductivity of the subsurface, in a fast and easy way, is by means of conductivity meters using the electromagnetic induction (EMI) principle. EMI methods can be used for a wide range of applications and notably to soil mapping, contaminants detection, characterization of shallow aquifers and location of buried objects or ore bodies. The EMI equipment consist basically of a primary magnetic field transmitter and, depending on the brand, a single or a set of magnetic field receivers. Measurements can be performed in several coil configurations but the two mostly used are the vertical and horizontal dipoles modes.

McNeill (1980) described the basic principles of the EMI method using electromagnetic dipoles with fixed source-receiver distance in the frequency domain and the concept of the relative and cumulative response functions. These functions have been widely used as a powerful tool for forward modelling and interpretation of measurements obtained by conductivity meters operating at low induction numbers for 1-D layered earth models. These well-known functions were derived and should be used for the instruments laid in the surface of the earth. The main goal of the present paper is to propose new generalized functions which can be used for instruments carried at any height from the surface.

Theory

Let us consider a homogeneous half-space on the surface of which an EMI equipment is located. We can consider that the half-space is formed by an infinite number of thin layers of thickness *dz* at depth *z* (here *z* denotes the depth of the thin layer normalized by the transmitter-receiver distance *s*). It is possible to calculate the secondary magnetic field in the receiver coil arising from the current flowing within any of these thin layers. Using the low induction number (LIN) approximation McNeill (1980) constructed a function $\Phi_V(z)$, for the vertical dipoles configuration as:

$$\Phi_V(z)=\frac{4z}{(4z^2+1)^{3/2}} \quad , \tag{1}$$

which describes the relative contribution arising from a thin layer at any depth *z* to the total secondary magnetic field in the receiver coil. From (1) we can derive that material located at a depth of $z=\sqrt{1/8}$ gives maximum contribution to the secondary magnetic field. It is interesting to note that the near-surface material (*z* close to zero) gives a very small contribution to the secondary magnetic field and therefore this coil configuration is quite insensitive to changes in near surface conductivity.

For the case of the horizontal dipoles configuration the function $\Phi_H(z)$ is given by:

$$\Phi_H(z)=2-\frac{4z}{(4z^2+1)^{1/2}} \quad . \tag{2}$$

Here the relative contribution from the near-surface material (z=0) is maximum and the response falls off monotonically with depth.

According to McNeill (1980), the construction of these response functions is possible because when using the LIN approximation one can assume that *"(i) all current flow is horizontal and (ii) all current loops are independent of all other current loops"*. As the definition of apparent conductivity, using the LIN approximation, is given in terms of the secondary magnetic field at the receiver, we can see that the functions Φ also give the relative contribution from material at different depths to the apparent conductivity read by the EMI instrument. The integral of either functions (1) and (2) from zero to infinity gives the total secondary magnetic field at the receiver coil from the entire half-space (note that as Φ is relative, the integrals of Φ are equal to 1) which is directly related to the electrical conductivity of the half-space. It is therefore possible to state with great precision the relative influence of material at different depths to the indicated apparent conductivity.

The functions Φ shown above are useful for describing the relative sensitivity of either of the two dipoles configurations to material at various depths. However a function derived from them is more

useful for performing calculations. It is defined as the relative contribution to the secondary magnetic field or apparent conductivity from all material below an assigned depth z and is given by:

$$R_{V/H}(z)=\int_{z}^{\infty}\phi_{V/H}(z)dz \quad . \tag{3}$$

It is called the cumulative response and can be written for vertical and horizontal dipoles modes as:

$$R_V(z)=\frac{1}{(4z^2+1)^{1/2}} \quad \text{and} \tag{4}$$

$$R_H(z)=(4z^2+1)^{1/2}-2z \quad . \tag{5}$$

Note that the above equations (1), (2), (4) and (5) were derived and are valid for the case where the instruments are laid on the surface of the ground.

Methodology

In this paper we calculated the functions Φ numerically by creating 1-D models consisting of a thin layer at depth z, with conductivity σ and thickness Δz surrounded by insulate material. We computed the off-phase component of the magnetic field using the full solution of Maxwell's equations for these 1-D models and divided it by the computed off-phase component of a homogeneous medium with conductivity σ. Alternatively, we converted the off-phase components into apparent conductivities of these 1-D models, using the methodology suggested by Andrade at al. (2016), and divided it by the conductivity of the homogeneous medium σ.

The electromagnetic forward modelling, based in the full solution of Maxwell's equations, for vertical and horizontal dipole source-receiver combination with an inter-coil separation $\boldsymbol{s}$ over an 1-D layered earth with N layers over an infinite half-space with conductivity σ_{N+1}, is given by Keller and Frischknecht (1966) in terms of the mutual coupling ratio (Q) which is the ratio between the secondary and the primary magnetic field at the receiver coil as:

$$Q^{VD}(s)=\frac{H^S}{H^P}=-s^3\int_0^{\infty}R_0(\lambda)J_0(s\lambda)\lambda^2e^{-2\lambda.h}d\lambda \quad \text{and} \tag{6}$$

$$Q^{HD}(s)=-s^2\int_0^{\infty}R_0(\lambda)J_1(s\lambda)\lambda e^{-2\lambda.h}d\lambda \quad , \tag{7}$$

where J_0 and J_1 are the first kind zero-order and first-order Bessel functions, λ is the radial wave number, h is the height of the dipoles from the ground and $R_0(\lambda)$ is called the reflection factor which depends on the thicknesses and the electrical conductivities of each layer and is calculated at the interface between the air and the first layer. It can be obtained recursively beginning with the bottom layer N observing that there are no upcoming waves from the lower half-space, so $R_{N+1} = 0$, and:

$$R_n(\lambda)=\frac{(\Gamma_n-\Gamma_{n+1})/(\Gamma_n+\Gamma_{n+1})+R_{n+1}e^{-2\Gamma_{n+1}d_{n+1}}}{1+(\Gamma_n-\Gamma_{n+1})/(\Gamma_n+\Gamma_{n+1})R_{n+1}e^{-2\Gamma_{n+1}d_{n+1}}} \quad , \tag{8}$$

where $\Gamma_n=\sqrt{\lambda^2+i\omega\mu_0\sigma_n}$, d_n and σ_n are the thickness and electrical conductivity of the n^{th} layer, μ_0 is the permeability of vacuum, ω is the angular frequency. $R_0(\lambda)$ is obtained assuming layer 0 as the air with $\sigma_0 = 0$. For a homogeneous earth case we just have to consider the model as composed by one single infinity layer with the conductivity of the ground, bellow an air layer with σ=0. The integrals in equations (6) and (7), the Hankel transforms of functions λ^2R_0 and λR_0, respectively, can be calculated by linear filtering. Here we used the Guptasarma and Singh (1997) filters with 120 elements for the Hankel J_0 transform and 140 elements for the Hankel J_1 transform. We tested both methods (off-phase ratio and apparent conductivity ratio), assuming h=0, for the technical specifications of several known brands of conductivity meters. Very good agreement between themselves and equations (1) and (2) were found even for conductivities up to 0.5 S/m, meaning that the tested instruments really operate at low induction numbers and it is therefore possible to use equations (1) and (2) with a very good accuracy.

To obtain generalized relative and cumulative response functions for the case of the instrument being operated at some height (h) from the surface of the ground we again used equations (6), (7) and (8). As an example, Figure 1 shows the results for the numerically calculated relative response functions

for the vertical dipole, using the specifications of the *GF Instruments CMD-Explorer* with s= 4.49m, with the instrument used at 1m above the ground (h=1m), for half-space conductivities of 0.5 and 0.001 S/m along with the plot of the relative response function at the surface (h=0) obtained by equation (1). We can see that the numerically obtained functions are quite the same for both conductivities. It is also found that these numerical functions at h=1m from the ground are almost entirely equal to the analytical expressions from equation (1) (h=0) shifted to the left in the *z-axis* direction and scaled by a constant factor $\boldsymbol{F}$. It is obvious to deduce that the shift in the *z-axis* direction is equal to the height (h) of the equipment from the ground (normalized by s), as the instrument, when raised from the ground, is *shifted* by h in the opposite direction of the *z-axis*.

To obtain the scale factor $\boldsymbol{F}$, let's denote the blue hatched area in Figure 1 as $\boldsymbol{A_1}$, which by definition must be equal to 1 (Note that in the figure the functions are only shown up to z=2, but $\boldsymbol{A_1}=1$ for $z \rightarrow \infty$) and the pink area as $\boldsymbol{A}$, which is also by definition equal to $\boldsymbol{R_V(h/s)}$ given by equation (4). As said before these two areas are related by $\boldsymbol{F}$ so that we can write $\boldsymbol{A_1 = A \cdot F \rightarrow R_V(h/s) \cdot F = 1}$ and finally we obtain $\boldsymbol{F = 1/R_V(h/s)}$. It can be shown that this is also valid for the horizontal dipoles configuration.

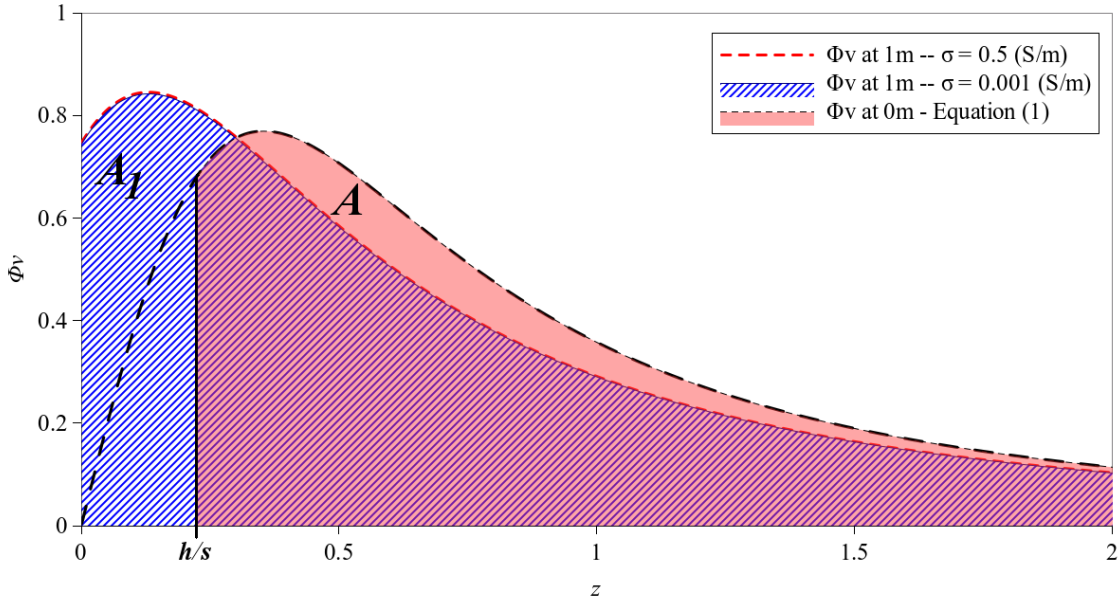

Figure 1 *Relative response function according to equation (1) and numerically calculated for the CMD-Explorer specifications (s=4.49m) at 1m above the ground and two different conductivities.*

Therefore, if the equipment is measuring at some height h from the surface, the generalized relative response functions can be obtained by adding the shift (h/s) to z in equation (1) and (2) and multiplying them by the factor $\boldsymbol{F}$, as :

$$\Phi_V(z,h)=[4(h/s)^2+1]^{1/2}\frac{4(z+h/s)}{[4(z+h/s)^2+1]^{3/2}} \quad \text{and} \tag{9}$$

$$\Phi_H(z,h)=\left(2-\frac{4(z+h/s)}{[4(z+h/s)^2+1]^{1/2}}\right)\frac{1}{[4(h/s)^2+1]^{1/2}-2h/s} \tag{10}$$

Integrating equations (9) and (10) using equation (3) one obtains the cumulative response functions for the generalized case . It occurs that they are also shifted and scaled in the same way as the relative response functions and are given by:

$$R_V(z,h)=\frac{[4(h/s)^2+1]^{1/2}}{[4(z+h/s)^2+1]^{1/2}} \quad \text{and} \tag{11}$$

$$R_H(z,h)=\frac{[4(z+h/s)^2+1]^{1/2}-2(z+h/s)}{[(4(h/s)^2+1)]^{1/2}-2h/s} \quad . \tag{12}$$

In Figure 2 we show, as examples, the functions $\Phi_{V/H}(z,h)$ and $R_{V/H}(z,h)$ for all the *CMD-Explorer* possible configurations operated at 1m from the ground. It is interesting to note that, based on the analysis of the $\Phi_V(z,h)$ function, that when using the equipment at some height h from the ground, the influence of near surface material (z=0) increases as the ratio (h/s) increases up to h/s=0.5. Then it decreases for larger values of this ratio when the curves behave very similarly as the relative response function for the horizontal dipoles configuration.

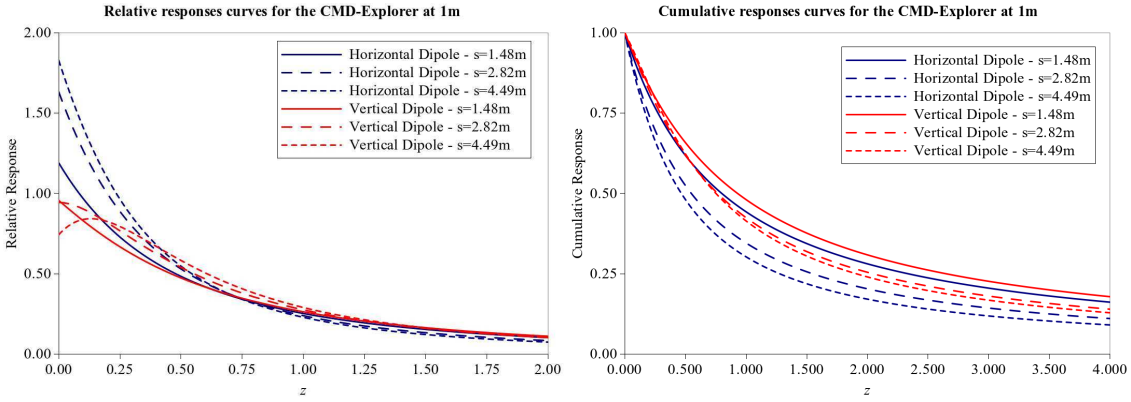

Figure 2 *Relative and cumulative responses curves for the 6 different CMD-Explorer configurations at 1m from the ground.*

Linear regressions between the numerically obtained response functions and the algebraic expressions (9-12) show almost perfect agreement with coefficients of determination (R^2) and slopes terms equal to 1 and intercept terms equal to 0 up to the sixth decimal place for all the studied instrument specifications and conductivities smaller than 0.5 mS/m.

Conclusions

We have shown that the well-known relative and cumulative response equations for electromagnetic induction instruments, operated on surface of the ground, can be used for several brands of conductivity meters operating at low induction numbers as they show a very good agreement with numerically calculated response functions by the full solution of Maxwell's equations. We have obtained generalized analytical expressions for the relative and cumulative response functions for the case when the instruments are operated at any height from the ground, which also showed almost exact agreement with the numerically calculated response functions for instruments operating at low induction numbers.

References

Andrade, F.C.M., Fischer, T. and Valenta, J. [2016]. Study of errors in conductivity meters using the Low Induction Number approximation and how to overcome them. *EAGE - Near Surface Geoscience*, Barcelona, Spain, Extended Abstracts.

Guptasarma, D. and Singh, B. [1997] New digital linear filters for Hankel J_0 and J_1 transforms. *Geophysical Prospecting*, **45**, 745–762

Keller, G. and Frischknecht, F. [1966] Electrical methods in geophysical prospecting. *International series of monographs in electromagnetic waves. Vol. 10*. Pergamon Press, Oxford, New York.

McNeill, J.D. [1980] Electromagnetic terrain conductivity measurement at low induction numbers. *Geonics Limited Technical Note TN-6*, Ontario.